The 2009 IEEE/RSJ International Conference on
Intelligent Robots and Systems
October 11-15, 2009 St. Louis, USA

GPS-based Position Control and Waypoint Navigation System for Quadrocopters

T. Puls, M. Kemper, R.Küke, and A. Hein, *Member, IEEE*

Abstract— **Motivation for the investigation of position and waypoint controllers is the demand for Unattended Aerial Systems (UAS) capable of fulfilling e.g. surveillance tasks in contaminated or in inaccessible areas. Hence, this paper deals with the development of a 2D GPS-based position control system for 4 Rotor Helicopters able to keep positions above given destinations as well as to navigate between waypoints while minimizing trajectory errors. Additionally, the novel control system enables permanent full speed flight with reliable altitude keeping considering that the resulting lift is decreasing while changing pitch or roll angles for position control.**

In the following chapters the control procedure for position control and waypoint navigation is described. The dynamic behavior was simulated by means of Matlab/Simulink and results are shown. Further, the control strategies were implemented on a flight demonstrator for validation, experimental results are provided and a comparison is discussed.

Index Terms— **UAS, UAV, control, VTOL aircraft, GPS, navigation**

I. Introduction

It is foreseen that there will be a future market for intelligent service and surveillance robots, capable of discreetly penetrating confined spaces and maneuvering in those without the assistance of a human pilot tele-operating the vehicle. Thus, the development of small autonomous aerial vehicles for outdoor and urban applications, which are able to perform agile flight maneuvers, is of significant importance. Such vehicles can also be used for establishing ad-hoc networks or in environments where direct or remote human assistance is not feasible, e.g. in contaminated areas or in urban search and rescue operations for locating earthquake-victims. Especially the abilities hovering above a given fixed position and maneuvering with high agility at low speed are essential for the mentioned applications. For this reason it was decided to investigate four rotor vertical takeoff and landing (VTOL) helicopters instead of fixed-wing aircrafts.

A. Problem description

Besides the challenge of keeping such inherently unstable systems in the air [1], one of the main problems is the ability to maneuver and hover autonomously without the interaction of a human pilot [2]. Thus it is desired to apply a controller enabling hovering and agile maneuvering without switching between appropriate flight-modes. Additionally the controller must be able to compensate constant wind conditions as well as temporary gusts. Thus, a further requirement is the ability to minimize trajectory errors while moving between waypoints (*zero cross-track angle control*), because it is unacceptable that a UAV leaves a given track, especially in urban scenarios. Furthermore it must be ensured that the UAV does not leave a commanded altitude. This may occur when abruptly changing the attitude of UAV with huge command values. In consequence the maximum thrust of the motors is not sufficient to keep UAV's altitude constant and, headwind conditions also cause height losses in addition. However, flying at maximum speed is desired due to limited operation-time of VTOL-missions. In consequence, along-track errors have to be minimized during waypoint navigation – along-track error damping is required.

Another precondition for reliable position control is an efficient altitude controller. The altitude controller in [4] was modified for application in the simulations and on the demonstrator. The used altitude controller is described in [15].

II. State Of The Art

In [8] and [9] the control and navigation principles of classical fixed wing aircrafts are well described, including problems of waypoint navigation and zero cross-track angle control. But these solutions cannot directly be adapted to 4 rotor helicopters due to the under-actuation and different configuration of 4 rotor helicopters [3].

There are publications regarding modeling and control of 4-rotor helicopters such as [1] and [3] but the authors mainly provide different types of attitude controllers and primarily not position controllers. In the recent past researchers investigate position control of VTOL for indoor applications. For example, in [11] a position controller based on monocular vision has been implemented and tested indoors. The quad-rotor helicopter was able to hover above a position within a range of around 1m. Although in [10] a PID-position controller was implemented, able to keep an indoor position of a 4 rotor VTOL within a range of 40cm or behavior-based navigation is investigated [5], the outdoor navigation of 4-rotor VTOL is still challenging, cf. the previous chapter.

Wendel et al. [6] describe the ability of combining the Inertial Measurement Unit (IMU) with Global Positioning System (GPS) to enable the acquisition of accurate position information. Additionally, the authors describe the stabilization of VTOL system with and without GPS. Navigation between different waypoints is undisclosed. [12] deals with trajectory planning of a 4 rotor helicopter in GPS-denied environments. A Belief Roadmap algorithm was used to plan trajectories in indoor environments.

In [13] a semi-autonomous "position hold" algorithm and waypoint navigator is presented. The procedure does not consider disturbances e.g. that UAV could be pushed away from a track or can lose height during flight. Further, the controller is not designed to fly at the maximum possible speed.

III. Target System

Figure 1 shows a photograph of the 4 rotor helicopter presented in real flight. It was used to test and verify the developed position controller.

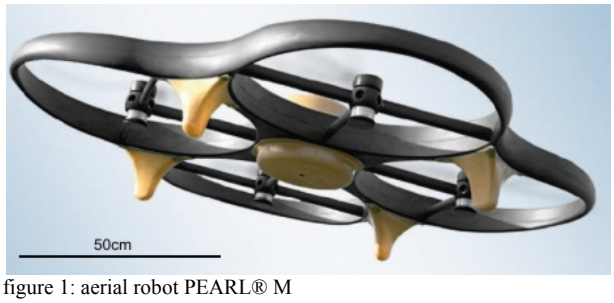

figure 1: aerial robot PEARL® M

The aerial vehicle is composed of an airframe, which consists of glass-fibre, carbon and Kevlar. The design focuses on low weight, stiffness and, on protecting the environment from the fast rotating and sharp rotor blades. The dimensions of the airframe are 110 cm x 110 cm x 20 cm. Due to the take-off weight of approx. 3 kg the system is equipped with four motor-rotor combinations able to lift up to 1.7 kg each. Thus, the system is able to carry an additional payload of 1 kg and still has got sufficient thrust to maintain its agility. A motor-rotor combination consists of a brushless motor, a suitable rotor and a motor controller.

A. Sensors

The system is equipped with sensors in order to measure and calculate the current pose of the UAV, particularly three gyroscopes for the angles φ, θ, ψ three accelerometers for *x, y, z* (cf. figure 2) and three magnetic field sensors. These sensors are primarily used to detect the attitude of the system. Due to their inherent inaccuracy and drift-behavior these sensors are not sufficient to calculate the position in all three dimensions, so that additional sensors are necessary. Hence a barometer is implemented to correct the calculated height and a GPS receiver is applied to detect the position. This paper does not deal with the question how to detect and calculate a precise geodesic position via GPS (see [6], [7]), for real-time constraints raw GPS data are considered for test purposes.

B. Attitude Controller

The attitude controller developed in [3],[4] for the angles φ (roll), θ (pitch) and ψ (yaw) was implemented on the target system. Due to the under-actuation of the 4-rotor helicopter every position change leads to an adjustment of the roll and pitch angles φ and θ.

IV. Theoretical Foundations

An example of the theoretical modeling of 4-rotor helicopters is shown in figure 2, with the initial body-fixed frame in the geometric centre. The orientation of the body can be described by a rotation *R* body-fixed *f* → inertial *g* [4].

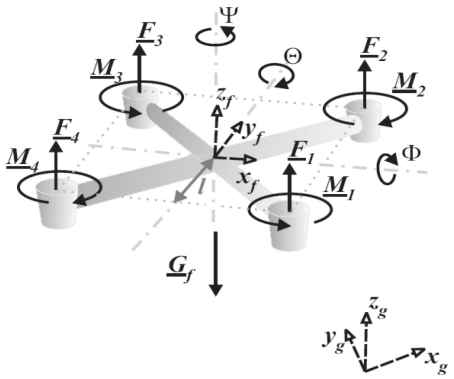

figure 2: System with Force and Torque Control

By means of this model the three rotational and the three translational differential equations of the system can be derived. The following equations are the basis for the development of the position controller.

$$I_{xx} \cdot \ddot{\varphi} = l \cdot (u_2 - c_{D4} \cdot \dot{\varphi}^2) - (I_{xx} - I_{yy})\dot{\theta}\dot{\psi} + \dot{\theta} \cdot I_z^{rot} \cdot \Omega_z$$
$$I_{yy} \cdot \ddot{\theta} = l \cdot (u_3 - c_{D5} \cdot \dot{\theta}^2) - (I_{yy} - I_{zz})\dot{\psi}\dot{\varphi} + \dot{\varphi} \cdot I_z^{rot} \cdot \Omega_z$$
$$I_{zz} \cdot \ddot{\psi} = u_4 - c_{D5} \cdot \dot{\psi}^2 - (I_{yy} - I_{xx})\dot{\varphi}\dot{\theta}$$

equation system 1: rotational equations

$$\begin{aligned} m \cdot \ddot{x}_g &= u_1 \cdot (\cos\varphi \sin\theta \cos\psi + \sin\varphi \sin\psi) \\ &\quad - c_{D1} \cdot \dot{x}_g^2 - (w_y \dot{z}_g - w_z \dot{y}_g) \\ m \cdot \ddot{y}_g &= u_1 \cdot (\cos\varphi \sin\theta \cos\psi - \sin\varphi \sin\psi) \\ &\quad - c_{D2} \cdot \dot{y}_g^2 - (w_z \dot{x}_g - w_x \dot{z}_g) \\ m \cdot \ddot{z}_g &= u_1 \cdot (\cos\varphi \cos\theta) - mg \\ &\quad - c_{D3} \cdot \dot{z}_g^2 - (w_x \dot{y}_g - w_y \dot{x}_g) \end{aligned}$$

equation system 2: translational equations

where *I* is the symmetric and constant inertial tensor, *l* the distance between rotor and centre, *m* the mass of the system, u_i the inputs (forces respectively torques) and c_{Di} the coefficients of drag. [3]

V. Position Control Algorithm

This section focuses on the 2D position control algorithm. The motor controllers, position control, attitude as well as altitude control are calculated with 120 Hz. Admittedly the GPS receiver only provides new data with a frequency of 5Hz but this algorithm can handle the height loss problem as well. Yet before the controller can be described one part regarding the height controller should be noted. The maximum allowed thrust in order to regulate the altitude is limited, so that there has to be a thrust-reserve for the attitude controller to be able to work properly. Thus, this maximum allowed thrust depends on the maximum velocity the UAV can achieve. Further, it depends on the wind-conditions and the maximum allowed attitude angles.

Hence, the controller performs calculation of the desired angles θ_d and φ_d by means of the bearing angle ω with respect to the geographic north and the distance d (in meters). These two values are directly computed from longitudes and latitudes provided by the GPS receiver, cf. [14]. The aim of this controller is to keep the UAV on a given track, which is defined by a start position *sp* and a target position *tp* (see figure 3). θ_c, φ_c and ψ_c are the current attitude angles of the UAV.

A. Zero cross track angle control

As soon as a new waypoint is defined the new start values ω and d are stored in ω_{start} and d_{start}. In addition the slope m_b and the *y*-intercept b_b of a linear function are calculated by

$$m_b = \frac{(pot-1)}{(d_{start}-d_0)}, 0 < pot \leq 1 \; and \; 0 < d_0 < d_{start}$$
$$\text{and } b_b = pot - m_b * d_{start},$$

where *pot*[1] defines the maximum allowed adjustment angle, i.e. the direct heading of the UAV towards the track, and d_0 is the desired distance the UAV should directly head to the destination.

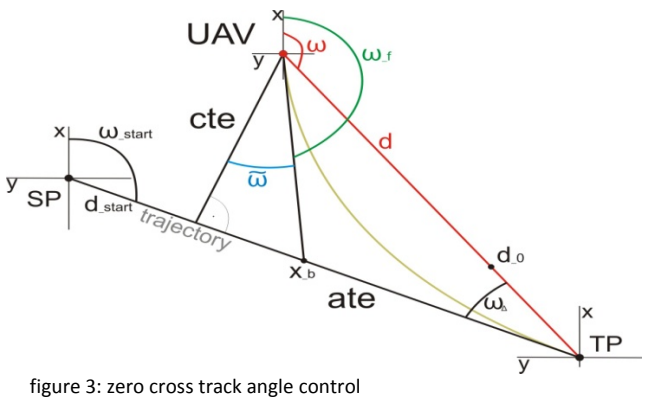

figure 3: zero cross track angle control

As soon as the UAV leaves the track and the distance to the target has exceeded the determined value d_0, the bearing angle ω will be adapted with respect to d. To satisfy this requirement the angle difference ω_Δ between the start bearing ω_{start} and ω is being calculated.

$$\omega_\Delta = \omega_{start} - \omega$$

In addition the along-track error *ate* and the cross-track error *cte* are being computed whereas the cross track error is defined as the distance between the UAV and the track and the along-track error as the distance to the target on the trajectory.

$$ate = d \cdot \cos \omega_\Delta$$
$$cte = d \cdot \sin \omega_\Delta$$

Hence, the adjustment angle $\tilde{\omega}$ is being calculated.

$$\tilde{\omega} = atan2(ate \cdot x_b, cte)$$

where x_b defines the point on *ate* the UAV should head to with

$$x_b = b_b + m_b \cdot ate$$

with $pot \leq x_b \leq 1$.

Lastly, the final bearing angle ω_f can be calculated by

$$\omega_f = \omega - ((\pi - \omega_\Delta) - \tilde{\omega}).$$

Due to the fact that the current yaw angle ψ_c must be considered ω_f is corrected by

$$\omega_\psi = \psi_c - \omega_f$$

B. PI Controller

At first the angles θ_d and φ_d are calculated for the first time by an adapted PI controller with the parameters k_p and k_i^x and k_i^y.

$$\varphi_d = \sin(\omega_\psi) * max(k_p \cdot d, \varphi_d^{max}) \cdot h_{loss}$$
$$\theta_d = \cos(\omega_\psi) * max(k_p \cdot d, \theta_d^{max}) \cdot h_{loss}$$

where $h_{loss} = \begin{cases} \frac{1}{(e_h - (e_h^{err}-1))}, e_h > e_h^{err} \\ 1, else \end{cases}$ is a term to antagonize the height loss problem with $e_h^{err} > 1$.

$$\varphi_d = \varphi_d - \left(-\sin(\psi_c) \cdot \left(k_i^x \int d_x \, dt + y_x^{cross}\right) + \cos(\psi_c) \cdot \left(k_i^y \int d_y \, dt + y_y^{cross}\right)\right)$$

$$\theta_d = \theta_d + \left(\cos(\psi_c) \cdot \left(k_i^x \int d_x \, dt + y_x^{cross}\right) + \sin(\psi_c) \cdot \left(k_i^y \int d_y \, dt + y_y^{cross}\right)\right)$$

After that, φ_d and θ_d have to be limited again with respect to the direction by:

$$\varphi_d = \varphi_d \cdot \left(\varphi_d^{max} / \left|\underline{W_d}\right|\right), \text{ if } \left|\underline{W_d}\right| > \varphi_d^{max}, \text{ with } \underline{W_d} = \begin{pmatrix}\varphi_d \\ \theta_d\end{pmatrix},$$

θ_d analogously.

During a track flight it is distinguished between two different states. If $k_p \cdot d = \varphi_d^{max}$, it is assumed that the UAV is on a transition flight, else it is close to the target. During transition flight the integral part is not adapted but an additional cross-track error proportionality is added.

- track flight

$$y_x^{cross} = \sin(\omega_{start}) \cdot k_p^{cross} \cdot cte$$
$$y_y^{cross} = \cos(\omega_{start}) \cdot k_p^{cross} \cdot cte$$

with $k_p^{cross} < k_p$.

[1] *pot* = point on track
e.g.: *pot = 1* means always direct to target and
pot = 0 means direct to track if $d \geq d_{start}$

If $(k_p \cdot d < \varphi_d^{max}) \Rightarrow y_x^{cross} = y_y^{cross} = 0$

- calculation of integral part

Only in close range of the destination the integral part of the controller is used to eliminate a steady state deviation from the desired position. But in contrast to a classic I-controller the parameter k_i is not constant. It varies regarding the moving direction.

$$k_i^x = \begin{cases} k_{ih}^x, d_x \cdot \dot{x}_c < 0 \\ k_{il}^x, else \end{cases} \text{ and } k_i^y = \begin{cases} k_{ih}^y, d_y \cdot \dot{y}_c < 0 \\ k_{il}^y, else \end{cases}$$

With $d_x = \cos(\omega_f) \cdot d$ and $d_y = \sin(\omega_f) \cdot d$ and $k_{ih} > k_{il}$.

As the angles θ_d and φ_d the integrals have to be limited, either with respect to the direction by

$$\int d_x\, dt = \int d_x\, dt \cdot \left(\varphi_d^{max} / \left| \underline{\int d\, dt} \right| \right)$$

if $\left| \underline{\int d\, dt} \right| > \varphi_d^{max}$, and with $\underline{\int d\, dt} = \begin{pmatrix} \int d_x dt \\ \int d_y dt \end{pmatrix}$, $\int d_y\, dt$ analogously.

Due to the reason, that the integral part is not adapted while cruising on a transition flight, it may happen the target position cannot be reached under changing weather conditions. Thus the following term was added to the controller and is calculated with the frequency of 120Hz.

$$\overline{\int d\, dt} = \overline{\int d\, dt} \cdot 0.99$$

if $\left| \underline{W_d} \right| < \varphi_d^{max}$ and $k_p \cdot d = \overline{\varphi_d^{max}}$.

C. Damping

The damping is the most important term to stabilize the UAV on a position, because a 4-rotor-helicopter is an under-actuated system with almost no internal damping characteristics. Hence, three different kinds of damping are added to the controller: The along-track velocity-damping ATSD, the cross-track velocity-damping and the acceleration-damping AD. Where ATSD is variable and CTSD and AD are constant. That means φ_d and θ_d are adapted by:

$$\varphi_d = \varphi_d - \left(\sin(\omega_\psi) \cdot ATSD + \cos(\omega_\psi) \cdot CTSD\right) - \left(\sin(\omega_\psi) \cdot AD_x + \cos(\omega_\psi) \cdot AD_y\right)$$

$$\theta_d = \theta_d - \left(\cos(\omega_\psi) \cdot ATSD - \sin(\omega_\psi) \cdot CTSD\right) - \left(\cos(\omega_\psi) \cdot AD_x - \sin(\omega_\psi) \cdot AD_y\right)$$

and must be limited again with respect to the direction by $\varphi_d = \varphi_d \cdot \left(\varphi_d^{max} / \left| \underline{W_d} \right| \right)$, if $\left| \underline{W_d} \right| > \varphi_d^{max}$, θ_d analogously.

- Velocity damping

It must be distinguished between ATSD and CTSD due to the reason that a damping towards the target is not desirable while being on transition flight. However, close to the destination the full damping should be available in any direction.

Hence, the parameter k_{ATSD} is dynamic with respect to d with:

$$k_{ATSD} = \begin{cases} 0, d > d_{max} \\ CTSD, d < d_{min} \\ m_c \cdot d + b_c, else \end{cases}$$

with $m_c = \frac{CTSD}{d_{min} - d_{max}}$, with $d_{min} < d_{max}$ and $b_c = CTSD - d_{min} \cdot m_c$.

The damping-terms can now be determined by:

$$ATSC = k_{ATSD} \cdot \cos(\omega_v) \cdot \left| \underline{v} \right|$$

$$CTSC = k_{CTSD} \cdot \sin(\omega_v) \cdot \left| \underline{v} \right|$$

with $\omega_v = \omega_f - atan2(\dot{y}, \dot{x})$ and $\underline{v} = \begin{pmatrix} \dot{x} \\ \dot{y} \end{pmatrix}$. k_{ATSD} and k_{CTSD} as control parameters.

- Acceleration damping

The damping is applied to antagonize abrupt disturbances. But the AD shall only impact the UAV during acceleration and not during deceleration. Thus AD is calculated as follows:

$$AD_x = \begin{cases} \ddot{x} \cdot k_{AD}, ((\dot{x} > 0) \wedge (\ddot{x} > 0) \vee (\dot{x} < 0) \wedge (\ddot{x} < 0)) \\ 0, sonst \end{cases}$$

AD_y analogously. k_{AD} is the control parameter.

VI. Simulations

Firstly, several simulations on Matlab/Simulink have been performed. This chapter presents some results. The flight dynamics of the 4-rotor-helicopter, i.e. the coupled system of six differential equations, have been implemented using Matlab/Simulink [3], [4]. The C-code of the implemented control system was embedded by means of a s-function into the simulation environment. Hence, successful validation can be performed by porting the code to the flight demonstrator.

A. Track Flight

Figure 4 shows a simulated flight of a 320 m track under wind conditions.

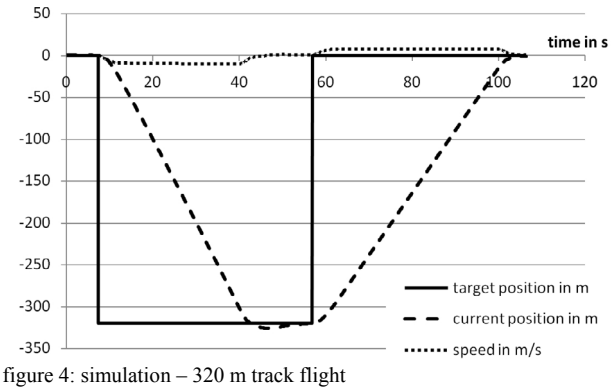

figure 4: simulation – 320 m track flight

The UAV was programmed to fly 320 m directly southbound and back to the starting point with a constant wind from north with a wind-speed of 2-3 m/s. As expected the wind leads to an increased velocity while flying southwards. Hence, the UAV overshoots the destination in the south.

B. Zero Cross Track Angle Control

Figure 5 shows the result of the zero cross-track angle control. The helicopters within the graphs are not true to scale.

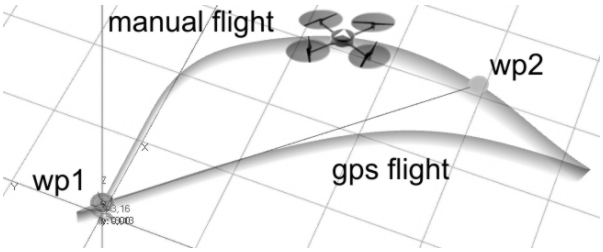

figure 5: simulation - zero cross-track angle control

The simulated flight was manually started at waypoint (wp) 1. The UAV was maneuvered along an arc with a velocity of 10 m/s to wp 2. As soon as the UAV reached this point, the position controller was switched on and wp 1 was set as its destination. It can be seen that the UAV tries to get back on track. The farther it is away from the destination, the stronger the UAV heads towards the track.

C. Simulcast Position and Altitude control

Figure 6 shows the simulation of the position controller in consideration of simulcast altitude alterations. The goal was to fly along a rectangle while simultaneously changing the desired altitude. No wind was considered during this simulation.

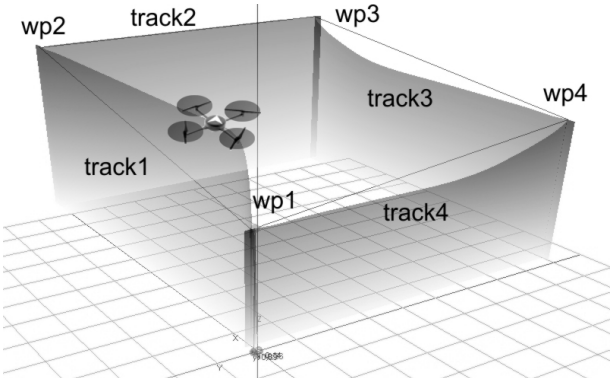

figure 6: simulation - rectangle

The first waypoint (wp 1) is located in a height of 30 m and is considered as starting position. After having reached the starting position, a simulcast position and altitude change has been sent. As can be seen in figure 6, the UAV first starts to compensate the altitude difference of 20 m. After that it is heading into the new position located 100 m north. This is the effect of the term h_{loss} of the position controller. The next waypoint 3 is located in the same height but 90 m east. Towards waypoint 4 again a simulcast position and altitude change was executed, but in this case the new height lay 10 m below the previous waypoint. This time the position and altitude difference is compensated simultaneously, because h_{loss} only takes effect if the desired height is higher than the actual. The last procedure of the simulation is similar to the stage before. From waypoint 4 back to the start position the desired height is again 10m lower.

VII. Experiments

This chapter provides the results of the experiment. The already in Matlab/Simulink implemented controller was ported to an ARM7 controller on the UAV. Then, the same test scenarios were flown as shown in the previous chapter. However the actual wind conditions were measured on ground and estimated for wind conditions in higher altitudes.

A. Track Flight

In figure 7 the real progress of the same 320 m track flight as previously described is shown.

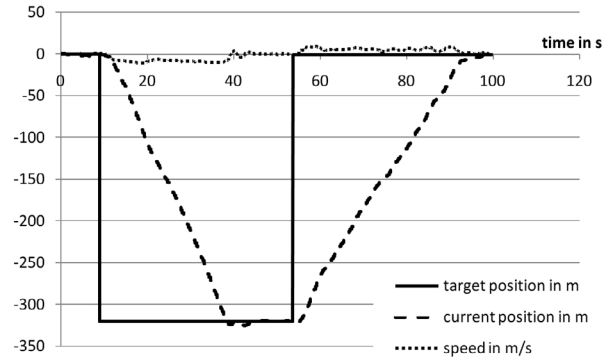

figure 7: experiment – 320 m track flight

The chronological sequence of the experiment in comparison to the simulation is almost the same. One difference can be found in the fluctuating velocity while flying from one waypoint to the other. This is due to wind gusts. Hence, there are some modifications of the bearing as effect of the "zero cross-track angle control".

B. Simulcast Position and Altitude control

In figure 8 the result of the experiment can be seen. The trajectories of the experiment and the simulations are similar. The differences base on the presence of wind (up to 5m/s measured on the ground) and additional gusts in the outdoor experiment. Thus, the integral part of the controller is built.

For example during flight from waypoint 1 to waypoint 2 the trajectory is different in the first section. During the height compensation phase, the UAV is pushed away by the wind because of the absence of the proportional part of the controller. Additionally, due to the integral effect of the controller, the UAV is moving away if increasing the thrust to gain height, i.e. the thrust vector is not straightly directed upwards while holding position

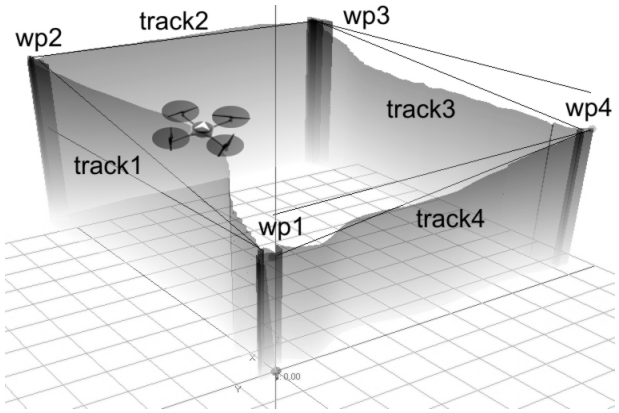

figure 8: experiment - rectangle

Further, it can be seen that the UAV tries to stay on track while moving from one waypoint to the other – as reaction on the wind conditions. Especially between waypoint 4 and 1 the UAV is blown away from its track and heads back towards it.

VIII. Conclusion

In this paper a control algorithm able to cover all requirements necessary for autonomously operating a VTOL UAV has been introduced. The developed controller was simulated and tested successfully in outdoor experiments. With this controller a 4 rotor helicopter is able to deal with constant wind up to 10m/s as well as with gusts. Furthermore, this controller can be applied to fly in urban scenarios due to its ability to fly along predefined tracks. Finally, with the novel control system the UAV is able to fly with the maximum possible speed without the risk of losing height during track flight.

The experiments were executed on basis of the GPS-data. Nevertheless this algorithm is sensor-independent.

IX. Outlook

During the simulation and experiments one became aware of some improvements.

The first problem occurred at heavy wind conditions, if the maximum allowed thrust and the maximum allowed attitude angles are not sufficient. Simply increasing the maximum allowed angle does not solve the problem adequately. The maximum allowed thrust has to be increased otherwise the UAV will not be able to maintain the actual altitude. Hence, a solution has to be found, so that the position errors do not increase. It has to consider maximum allowed thrust and angles with respect to the danger that there are not enough reserves for the attitude controller.

Another improvement would be the extension of the cross-track proportional part with an integral part to antagonize crosswinds better and to avoid permanent track errors.

Acknowledgment

This research activity was performed in cooperation with Rheinmetall Defence Electronics GmbH, Bremen and partialy sponsored by CART (competitive aerial robot technologies) research cluster in Bremen, Germany.

We would like to thank Hannes Winkelmann and Sönke Eilers for their continuous support and help. They greatly contributed to the simulation environment.

References

[1]S.Bouabdallah, P.Murrieri and R.Siegwart, *Design and Control of Indoor Micro Quadrotor, IEEE-International Conference on Robotics and Automation 2004,* New Orleans, USA, pp. 4393 – 4398.

[2]M. Kemper, M. Merkel and S. Fatikow: "A Rotorcraft Micro Air Vehicle for Indoor Applications", Proc. of 11th Int. IEEE Conf. on Advanced Robotics, Coimbra, Portugal, June 30 - July 3, 2003, pp. 1215-1220.

[3]M.Kemper, S.Fatikow: *Impact of Center of Gravity in Quadrotor Helicopter Controller Design*, in: Proc. of Mechatronics 2006, 4th IFAC Symposium on Mechatronic Systems, Heidelberg, Germany, September 12th - 14th 2006, pp. 157-162.

[4] M.Kemper, *Development of an Indoor Attitude Control and Indoor Navigation System for 4-Rotor-Micro-Helicopter*, Dissertation, University of Oldenburg, Germany, 02. Feb 2007.

[5]M.Mahn, M.Kemper: *A Behaviour-Based Navigation System for an Autonomous Indoor Blimp*, in: Proc. of Mechatronics 2006, 4th IFAC Symposium on Mechatronic Systems, Heidelberg, Germany, September 12th - 14th 2006, pp. 837-842

[6]Jan Wendel, *Integrierte Navigationssysteme,* Oldenbourg Wissenschaftsverlag GmbH, March 2007

[7]U-blox AG, *Essentials of Satellite Navigation,* Compendium Doc ID: GPS-X-02007-C, April 2007
Available: http://www.u-blox.com/customersupport/docs/GPS_Compendium(GPS-X-02007).pdf

[8]R.Brockhaus, *Flugregelung,* Springer Verlag, Berlin, 2. Auflage, neubearb. A. (Juli 2001)

[9]W.Rüther-Kindel, *Flugmechanik – Grundlagen und stationäre Flugzustände,* script ws 2006/2007, Available: http://www.tfh-wildau.de/ll05/3.Semester/Flugmechanik/

[10] G.M.Hoffmann, H.Huang, S.L.Waslander and C.J.Tomlin, *Quadrotor Helicopter Flight Dynamics and Control: Theory and Experiment, AIAA Guidance, Navigation and Control Conference and Exhibit,* 20-23 August 2007, Hilton Head, South Carolina, AIAA 2007-6461

[11] G.P.Tournier, M.Valenti and J.P.How, *Estimation and Control of a Quadrotor Vehicle Using Monocular Vision and Moiré Patterns, AIAA Guidance, Navigation and Control Conference and Exhibit,*21-24 August 2006, Keystone, Colorado, AIAA 2006-6711

[12] R.He, S.Prentice and N.Roy, *Planning in Information Space for a Quadrotor Helicopter in a GPS-denied Environment, IEEE International Conference on Robotics and Automation* (ICRA 2008), 19-23 May 2008, Pasadena Conference Center, Pasadena, CA, USA

[13] O.Meister, R.Mönikes, J.Wendel, N.Frietsch, C.Schlaile and G.F.Trommer, *Development of a GPS/INS/MAG navigation system and waypoint navigator for a VTOL UAV, SPIE Unmanned Systems Technology IX,* Volume 6561, pp. 65611D, 9-12.April 2007, Orlando, FL, USA

[14] B.Hofmann-Wellenhof, M.Wieser and K.Legat, *Navigation: Principles of Positioning and Guidance*, Springer Verlag, Wien, 1.Auflage, Oktober 2003

[15] T.Puls, H.Winkelmann, S.Eilers, M.Brucke and A.Hein, *Interaction of Altitude Control and Waypoint Navigation of a 4 Rotor Helicopter, German Workshop on Robotics* (GWR 2009), 09-10 June 2009, Braunschweig, Germany, *accepted*